Quantitative Interpretation of Magnetic Anomalies in Ebolowa-Djoum area (Southern Cameroon)

Marcelin Bikoro-Bi-Alou [1, 2*], *Theophile Ndougsa-Mbarga*[3*] *and Tabod Charles Tabod*[1]

[1]*Department of Physics, Faculty of Science, Univ. of Yaoundé I, P.O. Box 812, Yaoundé, Cameroon*
[2] *Department of Renewable Energy, Higher Institute of the Sahel, Univ. of Maroua, P.O. Box 46 Maroua, Cameroon*
[3]*Department of Physics Advanced Teachers' Training College, Univ. of Yaoundé I, P.O. Box 47 Yaoundé, Cameroon*

*Corresponding authors: theopndougsa@gmail.com/marcelinbikoro@yahoo.fr

Abstract

A quantitative interpretation of aeromagnetic data is conducted in the Ebolowa-Djoum area. The aim of the study is to estimate magnetic and geometrical parameters of the causative bodies using spectral analysis and 2.5 modeling. In addition an indicative evaluation of the volume of magnetic material is done using geoinformation mapping tool. The techniques are applied to three N-S profiles (P1, P2 and P3) that cross three anomalies at Kamélon (P1), Ngoa (P2) and between Djoum and Olounou (P3). The application of the techniques cited above has given the following results: (1) Magnetic bodies identified have susceptibility with a range that coincides to iron formations such as magnetite and haematite; (2) the depth to the top of the iron formation that produce the observed magnetic anomalies varies from 88 m to 109 m at Kamélon, 32 m to 670 m at Ngoa and 50 m to 580 m along the profile P3; (3) the depth to the foot of that formations is from 614 m to 1240 m at Kamélon, 802 m to 965 m at Ngoa and 250 m to 1340 m along P3; (4) an E-W extent (strike) of iron formations is 12000 m at Kamélon, 1600 m to 12000 m at Ngoa and 12000 m in the P3 profile; (5) a N-S extent (width) of iron formations ranging from 2390 m to 77470m at Kamélon, 3680 m to 9600 m at Ngoa and 1540 m to 13140 m in the P3 profile; (6) indicative volume value of that iron formations varies from 10.1 km^3 to 16.3 km^3 at Kamélon, 0.7 km^3 to 8.7 km^3 at Ngoa and 1.20 to 18.0 km^3 along profile P3.

Keywords: Magnetic anomalies, spectral analysis, 2.5D modeling, iron formation, indicative volume, Ebolowa-Djoum area

1   Introduction

The study area (Fig. 1a) is located in the southern Cameroon between 11°30'E and 13°E, and between 2°30'N and 3°N. The aeromagnetic data in this area has been collected by *Paterson et al.* (1976) who carried out a preliminary detailed interpretation to assess its iron ore potential. More recently, combined studies of geochemistry, geology and geophysics were conducted in the southeast of the previous area to estimate the mineral resources (*SRK,* 2011; *Ndougsa-Mbarga et al.,* 2013). Based on the knowledge
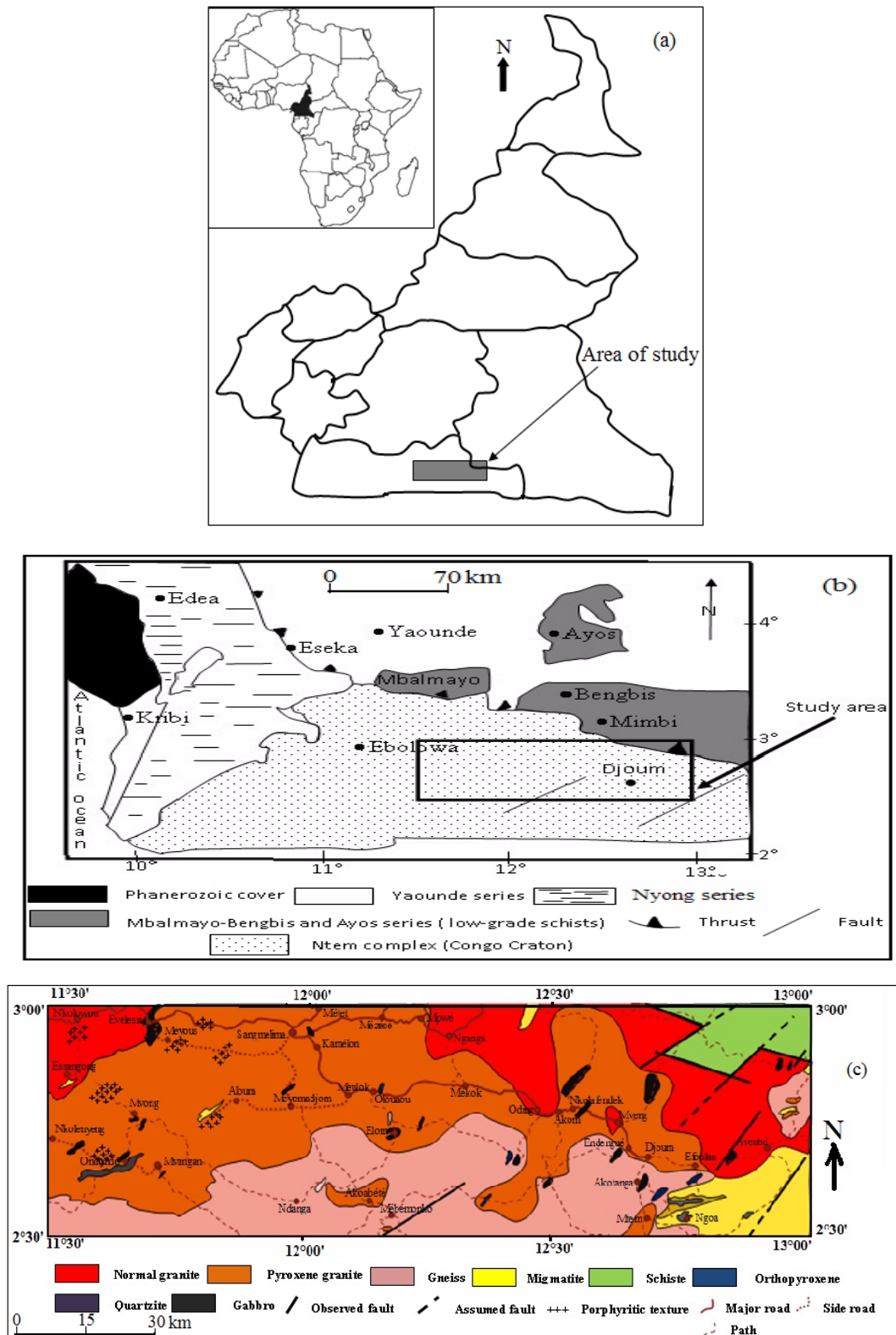
Fig. 1. (a) Location of the study area within Cameroon, (b) Geological sketch map of southern Cameroon showing its main lithological units and the location of Ebolowa-Djoum region (after *Olinga et al.,* 2010), (c) Geological sketch map of the study area showing its main lithological units (*Ndougsa-Mbarga et al.,* 2013).

of the previous work, this paper presents estimates to the depths to the top and to the foot of the magnetic bodies that produce magnetic anomalies in Kamélon, Ngoa and between Djoum and Olounou (Fig. 2).This paper also provides estimated of N-S and E-W extends, volume of the magnetic bodies and confirms their nature. For these achievements, two techniques are applied: the spectral analysis and 2.5D modeling. From the last one, the use of georeferencing GIS tool of the 2.5D models allows to determine the volume of different iron formations observed. The geology of the area suggests rocks with a high magnetic susceptibility that is useful for a good analysis of the magnetic anomalies observed on the *Paterson et al.* (1976) map.
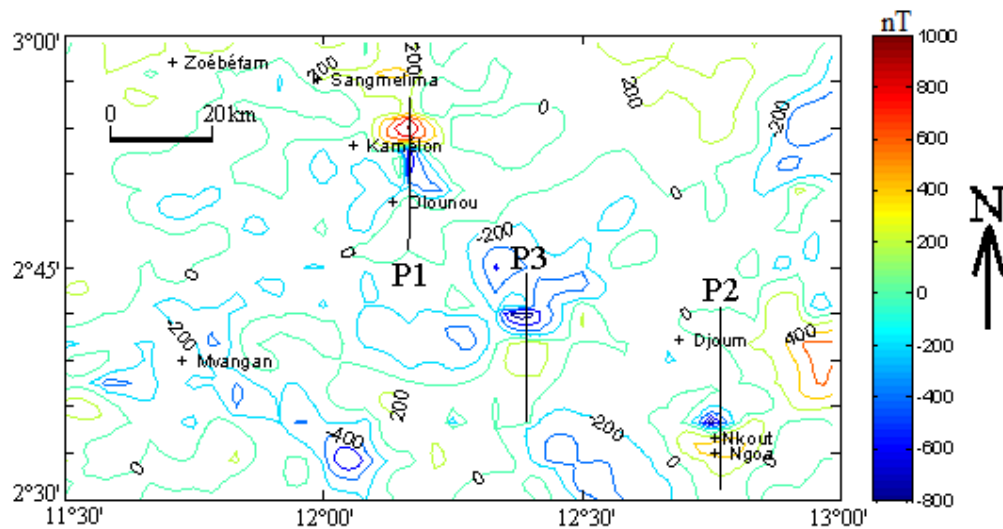

Fig. 2. Residual magnetic map of the study area (*Ndougsa-Mbarga et al.,* 2013) showing the location of P1, P2 and P3 profiles. Contour interval is 200 nT.

2   Geological setting

Geological mapping of the study area has been done by *Champetier de Ribes* (1956), and *Gazel & Guiraudie* (1965). The area is located towards the northern edge of the Congo Craton (Fig. 1b) which is one of the stable zones of Africa since the Catarchean (*Eno-Belinga*, 1984). The rocks of the area (Fig. 1c) are mainly gneisses and granites with gabbro, quartzite and orthopyroxene intrusions (*Paterson et al.,* 1976; *Tadjou et al.,* 2009). In the southeast of the study area, migmatites are described as quartzitic gneisses with localized occurrences of quartzite containing magnetite and haematite (*Paterson et al.,* 1976). The archean rock unit mentioned above belong to the Ntem Complex (Fig. 1b) that represents the north-westhern part of the Archean Congo Craton in Central Africa (e.g. *Bessoles and Trompette,* 1980; *Cahen et al.,* 1984). In the north-eastern part of the study area, granites are in contact by faults with chlorite schists of Mbalmayo-Bengbis series. The Kibarian Mbalmayo-Bengbis series (1800-1200 Ma), rejuvenated in the Pan-African tectonics (620±10 Ma) (*Penaye et al.,* 1993) is characterized by an epizonal metamorphism (*Nedelec et al.,* 1986; *Nzenti et al.,* 1988). The met-

amorphic rocks of the study area have an E-W trending (S1) foliation (*Suh et al.,* 2009). The S1 foliation has near vertical dip to the north and is locally deformed into mesoscopic isoclinal D2 folds (*Suh et al.,* 2009). The S2 foliation is a regional, steeply dipping planar fabric with a variable oriented stretching lineation, and large-scale open folds that are associated with N-S trending. This N-S trending is correlated to sinistral and dextral strike-slip faults and mylonitic (S3) foliation. The S2 foliation is well observed in greenstone units in the Ntem Complex (*Shang et al.,* 2004) and its development is linked to dome and basin tectonics related to diapiric movements (*Tchameni et al.,* 2001). During the Pan-African orogeny, a mobile belt known as the Yaoundé series (Fig. 1b), drifted southward and collided with the Ntem Complex (*Mvondo et al.,* 2007; *Toteu et al.,* 2004; *Olinga et al.,* 2010). Consequently, the Yaoundé series thrusted onto the Ntem Complex reactivating, under brittle-ductile conditions, NE to SW trending shear zones in the Ntem Complex (*Toteu et al.,* 2004*; Shang et al.,* 2004; *Suh et al.,* 2009). Those sheared areas seem to be a favorable environment for base metals mineralization, such as iron formation called bounded iron formations (BIF).

3   Data acquisition and filtering

The data set use in the present study is from an aeromagnetic survey covering some parts of Cameroon territory (*Paterson et al.,* 1976). This aeromagnetic survey was conducted in 1970 by Survair Limited (Ottawa) as part of a co-operative agreement between the Canadian and the Cameroon governments. The flying height was 235 meters, flight lines had a N-S direction with 750 meters interlines space and the recording sensitivity of the magnetometer used was more or less 0.5 nT (*Paterson et al.,* 1976). The final report of *Paterson et al.* (1976) was accompanied by magnetic maps. Aeromagnetic data interpreted in this paper were extracted from one of these maps covering the study area. The total magnetic field data were continued upwards to a height of 500 meters. Data within the study area was separated into regional and residual anomaly using finite element approach (*Ndougsa-Mbarga et al.,* 2013). This approach is widely used by several authors (*Mallick and Sharma,* 1997 &1999; *Kaftan et al.,* 2005; *Ndougsa et al.,* 2013) in the data filtering because it has the advantage to solve the problem of non uniqueness of the gravity or magnetic regional anomalies posed by other methods as polynomial methods; and it seems more objective, efficient and accurate (*Mallick and Sharma,* 1997 and 1999; *Kaftan et al.,* 2005).

As part of this work, three profiles have been plotted on the residual map obtained after the separation of the data (Fig. 2). Data collected along these profiles were used in spectral analysis and 2.5D modeling. In addition GIS was used to estimate the volume of the causative anomalous bodies.

4   Methods

The following section describes the methodology undertaken for modeling the causative bodies of the study area target anomalies. This study combines two methods

which are the spectral analysis and 2.5D modeling. The combination of many approaches is related to the fact that, an interpreter must understand the relationship between the form, amplitude of the magnetic response of a mineral deposit and other factors as the geometry, depth of the deposit, its orientation relative to magnetic north, and the inclination of the Earth's north at its location (*Gunn and Dentith,*1997).

4.1   Spectral analysis method

Spectral analysis has been widely used by several authors (eg. *Spector and Grant,* 1970; *Gerard and Debeglia,* 1975; *Bhattacharyya,* 1978; *Pal et al.,* 1978/79; *Njandjock et al.,* 2006; *Nguimbous et al.,* 2010) for depth determination of magnetic and gravity anomalies. Since the gravity and magnetic anomalies can be conveniently treated as space series amenable to Fourier analysis and synthesis (*Pal et al.,* 1978/79), without in any way affecting the intrinsic features of these anomalies, spectral methods provide a powerful approach to their analysis and interpretation. Spectral analysis does not require knowledge of the geometry, the density contrast or magnetic susceptibility of the causative bodies; it simply asks the study of power or energy spectrum as a function of wavelength or frequency. The power or energy spectrum of the anomaly will have dominant high frequency components when the anomaly is continued to the proximity of the source (*Pal et al.,* 1978/79). The near-surface sources will thus give flatter, and the deeper sources will give steeper, power spectrum (*Pal et al.,* 1978/79). The depth (h) of an interface can be obtained by using the *Gerard and Griveau* (1972) formula which is given below:

$$h = \Delta(LogE)/4\pi\Delta(n) \qquad\qquad (1)$$

Where E represents the energy spectrum; $\Delta(LogE)$ is the variation of logarithm of energy spectrum in the interval of frequency $\Delta(n)$.

Depths obtained by spectral analysis are then used as constraints in the modeling. The constraints are important because the magnetic method provides a plurality of solutions for inverse problems. To propose a unique and acceptable geophysical model, information arising from spectral analysis or Euler deconvolution (*Boukeke*, 1994) can provide constraints for the depth of the observed anomalies. In addition, available geological information or drilling data can provide constraints for material properties.

4.2   2.5D modeling

When a source of anomalies presents a preferred extension in a given direction, profiles are interpreted perpendicular to the main extension. If the longitudinal extend is at least five times greater than the transverse width, we assume infinite strike extent and the modeling is two-dimensional (2D) (*Talwani and Heirtzler,* 1964; *Grant and West,* 1965). If the ratio of main extension to transverse extension is smaller, modeling should take into account the limited length of the body. In that case modeling is called 2.5 dimensional (2.5D). Mag2dc (*Cooper,* 1997) is a 2.5D modeling program used in this pa-

per. This program uses a 2.5D Talwani's algorithm to calculate the magnetic field anomaly produced by the causative bodies (*Cooper,* 1997).

4.3   Material volume evaluation

From the 2.5D model, it is possible to estimate the volume of the perturbing mass. Indeed, the cross section of the model being the same along the longitudinal direction (*Cooper,* 1997), it is sufficient to multiply the cross section area with the strike extent of the model to get its volume.

The estimation of the surface of the area can be done by a suitable geoinformation tool package. For that purpose, we use MapInfo software. In this case, we must georeference the cross section of the model obtained from the 2.5D modeling, by assuming that it is superimposed on the Earth surface. This means that we rotate the model cross-section 90 degrees to project it on the Earth surface. According to the precision of the MapInfo tool, the error related to this operation cannot exceed 5% as stated by the GIS standards. In addition the 2.5 D model geometric parameters (strike, cross section) are known from the model obtained through the modeling, and this model is constrained by geological observations.

It's also important to recall that the estimation of the resource does not referred to the measured resources or proven reserve as stated by the international standards concerning the reporting of ore evaluation, but still being indicative evaluation (*Kerr et al.,* 1994).

5   Results

5.1   Spectral analysis

Three profiles P1, P2 and P3 (Fig. 3) were plotted in the study area. The energy spectrum of each profile presents two types of variations: rapid changes at the low frequencies and slow changes at mid and high frequencies (Fig. 4). For each energy spectrum, two straight-lines are plotted in the least square sense; the first straight-line for rapid changes and the second for slow changes. The application of the formula (1) gives following results:

    a) The depth to the shallowest interface of the target anomalies varies between 60 to 147 m.

    b) The depth to the deepest interface is between 866 to 1250 m. Table 1 below shows the results of theses depths per profile. The error related to the calculation of depth was set at 5% (*Nnange et al.,* 2000).
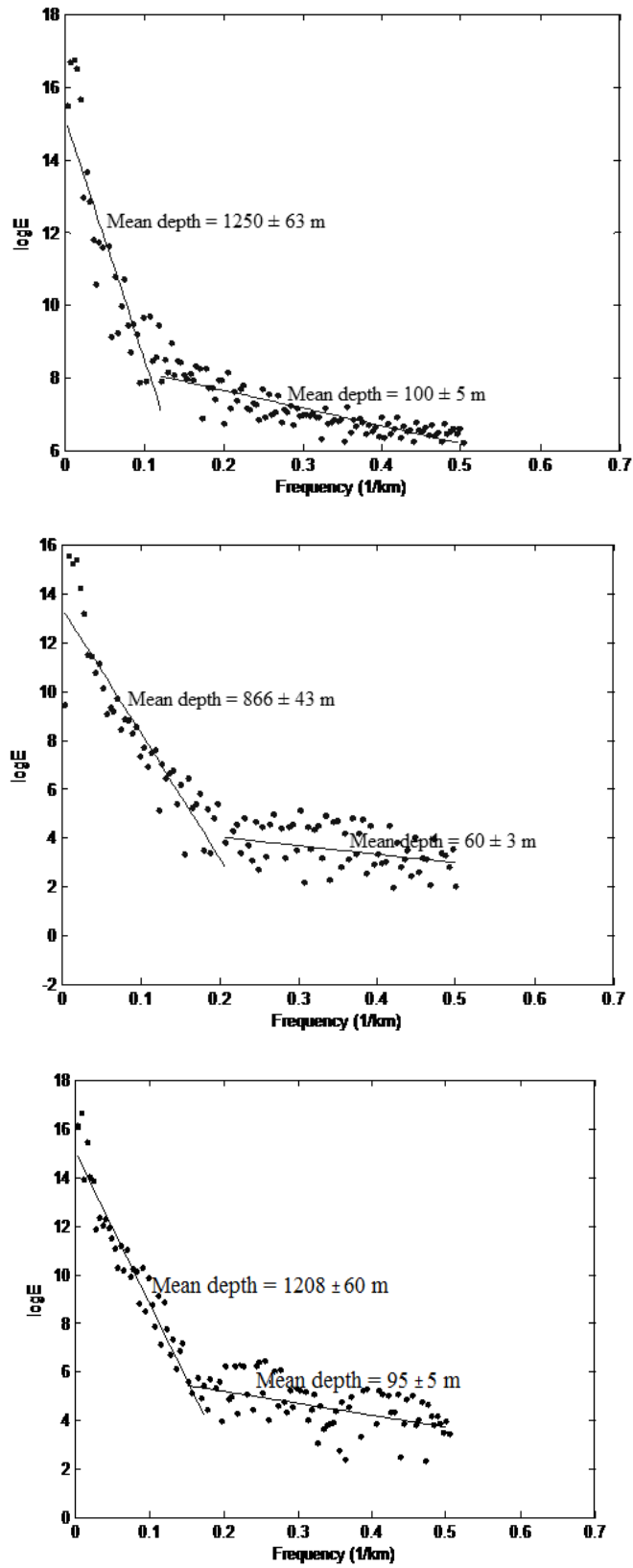
Fig. 3. Energy spectrum of (a) P1 profile, (b) P2 profile and (c) P3 profile; lines are fitted to the spectrum in the least square sense.

5.2   2.5D modeling

We used 32700 nT as total intensity, -18° as inclination and 6.2° as declination of the geomagnetic field. These values were extracted from isomagnetic maps of the 1970 IGRF's (International Geomagnetic Reference Field) model.

The obtained 2.5D models (Fig. 4) show magnetic bodies with variable geometrical and magnetic parameters.

Geometrical parameters of the magnetic bodies vary from profile to profile. Table1 summarizes for each profile the depth to the top, depth to the foot, and the strike and the width of each magnetic body. The lowest depth to the top of the models is17 m and corresponds to the body 4 from the P2 profile (Table 1). The very long bodies with an extent of 1200 m in the E-W direction are from the profile P3 (Table 1) and the body 4 from profile P2 (Table 1).

Table 1. Spectral analysis results and 2.5D models parameters of magnetic bodies from P1, P2, P3 profiles; k = Magnetic susceptibility, Z_T = Depth to the top, Z_B = Depth to the bottom, Z_S = Depth to the shallowest interface, Z_D = Depth to the deepest interface.

| Profile	2.5D models					Spectral analysis	
	Body	**k (SI×10⁻³)**	**Z_T (m)**	**Z_B (m)**	**E-W$_{extent}$ (m)**	**S-N$_{extent}$ (m)**	**Z_S (m)**	**Z_D (m)**
P1	1	501 ± 24	88 ± 4	1020 ± 51	2562 ± 128	12000 ± 600		
	2	260 ± 13	109 ± 5	1240 ± 62	2390 ± 120	12000 ± 600	100 ± 5	1250 ± 63
	3	221 ± 11	104 ± 5	614 ± 123	7740 ± 387	12000 ± 600		
P2	1	369 ± 20	32 ± 2	882 ± 44	5000 ± 250	10000 ± 500		
	2	729 ± 33	62 ± 3	822 ± 41	3680 ± 184	4000 ± 200	60 ± 3	866 ± 43
	3	128 ± 6	275 ± 14	965 ± 48	9600 ± 480	12000 ± 600		
	4	454 ± 22	670 ± 34	802 ± 40	4630 ± 232	1600 ± 80		
P3	1	343 ± 17	50 ± 3	540 ± 27	1540 ± 77	12000 ± 600		
	2	677 ± 27	540 ± 27	1330 ± 67	13140 ± 657	12000 ± 600		
	3	376 ± 20	130 ± 7	1340 ± 67	3700 ± 386	12000 ± 600		
	4	468 ± 23	170 ± 8	530 ± 27	8920 ± 446	12000 ± 600	95 ± 5	1208 ± 60
	5	172 ± 8	90 ± 5	1100 ± 55	12480 ± 624	12000 ± 600		
	6	53 ± 3	140 ± 7	250 ± 13	2600 ± 130	12000 ± 600		
	7	151 ± 7	290 ± 15	380 ± 19	3560 ± 178	12000 ± 600		
	8	39 ± 2	580 ± 29	670 ± 34	3760 ± 188	12000 ± 600		
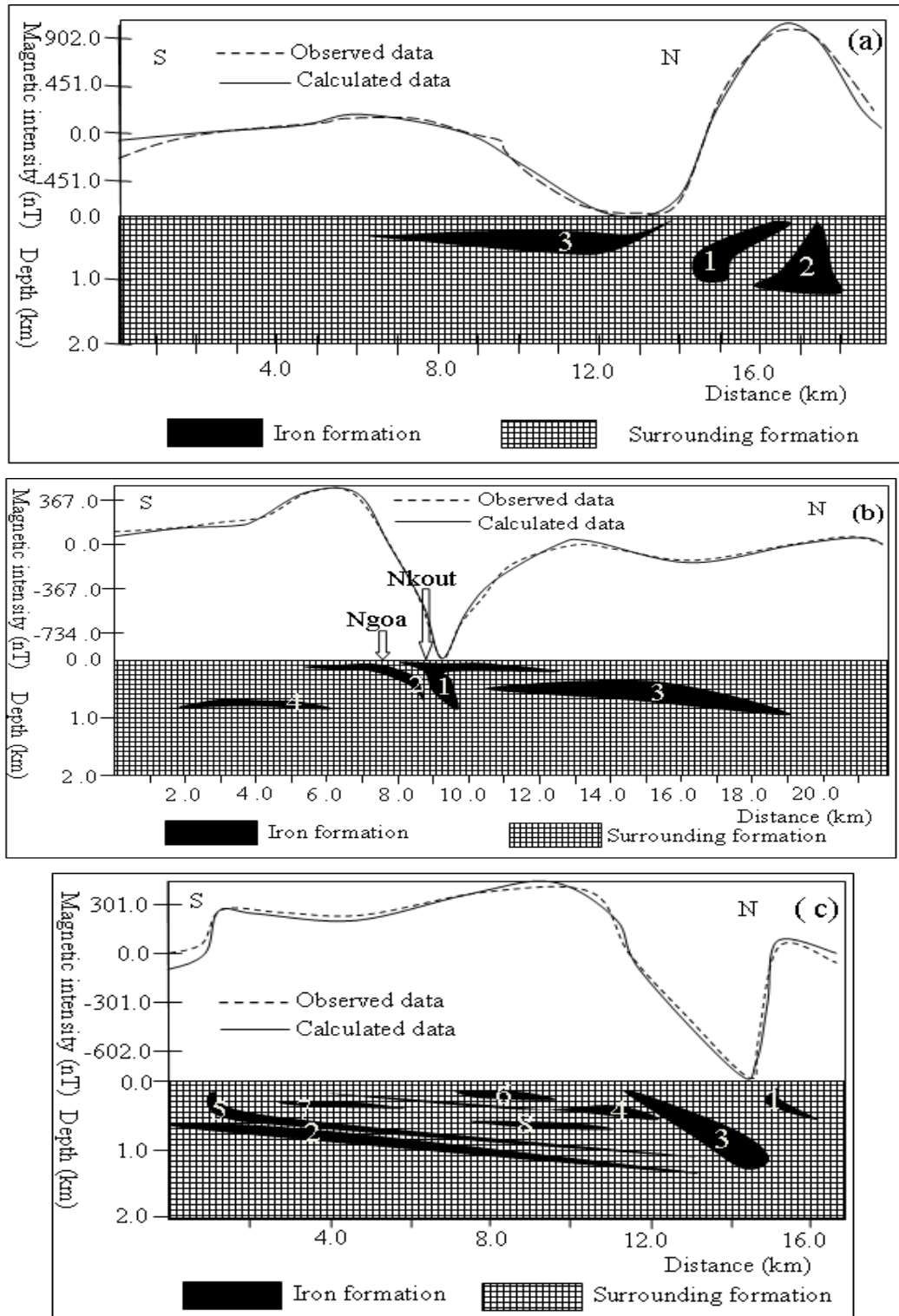
Fig. 4. Vertical cross-sections of the 2.5D models obtained for profiles P1 (a), P2 (b) and P3 (c); with the fit between measured data (dashed line) and computed field (solid line); the background represents the surrounding geological formations.

The magnetic susceptibilities of the bodies are also varying. In addition, their values are relatively weak for shallow bodies, high for deep formations and average for bodies with great depth extent. Table 1 shows the values of susceptibility for each profile and related bodies.

The susceptibility constraints used to obtain the 2.5D models has put in evidence the iron formations. The values found out are included in the range of 0.039 to 0.729 in IS units (Table 1).

5.3   Magnetic material volume evaluation

The estimated volume of the magnetic material from the 2.5D models was made possible by the calculation of cross section of the magnetic body. This calculation was done with MapInfo 7.5 software. The volume of a body is then the product of the cross section of that body by its E-W extension. This calculation as we recall above is based on the fact that, the 2.5D model geometric parameters are estimated from the observed model, and the derived evaluation of the resource is also an estimated one. Thus, the values of the volume vary from a profile to another (Table 2) as follow: (P1) from 10.1 to 16.3 km^3, (P2) from 0.7 to 8.7 km^3 and (P3) from 1.2 to 18 km^3. Those values have to be considered as indicative and can be ameliorated by a 3D modeling which integrates the fact that along one 2.5D modeling the neglecting of the variation of the strike extent introduces an underestimation/overestimation of some parameters value.

Table 2. Cross-section and indicative volume values of magnetic bodies from P1, P2 and P3 profiles.

Profile	Body	Cross section (km^2)	Volume (km^3)
P1	1	0.84 ± 0.01	10.1 ± 0.5
	2	1.12 ± 0.06	13.4 ± 0.7
	3	1.36 ± 0.07	16.3 ± 0.8
P2	1	0.87 ± 0.04	8.7 ± 0.4
	2	2.03 ± 0.10	8.1 ± 0.4
	3	0.43 ± 0.02	5.2 ± 0.3
	4	0.43 ± 0.02	0.7 ± 0.1
P3	1	0.13 ± 0.07	1.6 ± 0.1
	2	1.50 ± 0.08	18 .0 ± 0.9
	3	1.00 ± 0.05	12.6 ± 0.6
	4	0.10 ± 0.01	1.2 ± 0.1
	5	0.64 ± 0.03	7.68 ± 0.4
	6	0.19 ± 0.01	2.28 ± 0.1
	7	0.18 ± 0.01	2.16 ± 0.1
	8	0.30 ± 0.02	3.6 ± 0.2

6   Discussion

Magnetic susceptibilities obtained from the Mag2dc program are in the range of that corresponds to iron ore with magnetite and hematite. The comparison between the susceptibility values extracted from models (Table 1) and known susceptibility values of *Parasnis* (1997) for some iron ore such as magnetite and hematite, confirms a good correlation. The variation of the magnetic susceptibility in these models suggests that the modeled magnetic bodies are in general a mixture of iron ore formations. This assumption is justified by *SRK* (2011) report which describes the magnetic bodies in Nkout area (Fig. 4b) as banded iron formations (BIF) consisting of a mixture of magnetite and hematite.

The presence of relative weak magnetic susceptibility in shallow bodies and high values in depth reveals an abundance of weathered material in near surface and fresh iron formations in depth. This also means that weathered material in near surface is rich in hematite and fresh iron formations are rich in magnetite. *SRK's* (2011) analyses in the resources evaluation at Nkout area are in agreement with the statement mentioned above. The above correlation is also explained by the magnetite weathering process of the Nkout iron deposit (*Suh et al.,* 2009).

The body 1 from profile P2 is located at Nkout area (Fig. 4b), where drillings were realized in the eastern part (*SRK*, 2011). Indeed, coordinates of the Nkout point (Fig. 2) are 2°34'N and 12°46'E or 251671E and 283913N (UTM coordinates) and, coordinates of the most western drilling are 252560E and 285299N (*SRK*, 2011). That body has a northward steeply dipping with a 10000 m E-W extent and 882 m depth. It forms a vertical cross-section comparable to the SRK's cross-section block model of Nkout mineralization (Fig. 5). That block model was constructed on the basis of borehole and topography data available over of 8900 m E-W extent. With the E-W extent of the **body 1** from profile P2 we suggest that the Nkout mineralization goes beyond 8900 m of the SRK's block model strike.

Results derived from spectral analysis, may be interpreted here as the depth of the transitional zone that creates magnetic susceptibilities contrast. These transitional zones are between weathered and fresh iron formations in near surface and between fresh iron formations and surrounding basement in depth.

According to the body 1 from profile P2, the near surface transitional zone is at 60 m and the deepest transitional zone is at 866 m (Table 1). Boreholes from NKGS008 to NKDD022 (Fig. 5) show in the one hand that the near surface transitional zone is situated between 30.6 and 91.64 m and the deepest one is at 820 m in the other hand (*SRK*, 2011). From Table 1 we note that, the depth to the top (Z_T) of the body 1 from profile P2 is less than the depth of the near surface transitional zone. These both observations allows to assume that the thickness of obtained 2.5D models of magnetic bodies include the thickness of the weathered magnetized materials and the true thickness of fresh iron ore deposit.
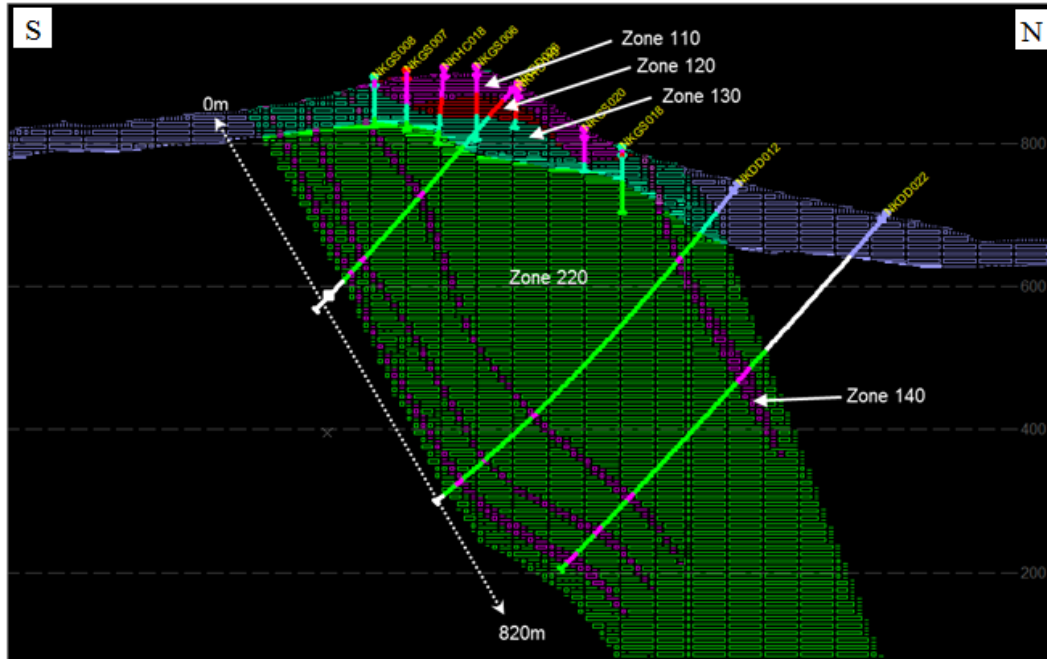
Fig. 5. Nkout empty block model cross section constructed on the basis of borehole and topography data available over of 8900 m E-W extent looking west; zones 110, 120 and 130 are geological domains of haematite rich material; zone 220 is a geological domain of magnetite rich material; zone 140 is a geological domain of oxidized metasediment (*SRK,* 2011); NKGS008, NKGS007, NKHC018, NKGS020, NKGS018, NKDD012, NKDD022 are boreholes identity.

7   Conclusion

In this paper, spectral analysis was used as constraints for 2.5D modeling and to estimate the average depth of transitional zones. In addition, the Mag2dc program allowed us to propose 2.5D models showing some magnetic bodies correlating with geological and drilling data tests of *SRK* (2011). The magnetic susceptibility values obtained are consistent with the nature of iron formations composed of magnetite and hematite. The 2.5D models have depth to the top between 88 and109 m at Kamélon (P1), 32 and 670 m at Ngoa (P2) and from 50 to 580 m between Djoum and Olounou (P3). The N-S and E-W extents of 2.5D models range respectively from 1540 to 13140 m and 1600 to 12000 m.

In addition, with constant cross sections derived from 2.5D models, the estimation of the indicative volume of the iron formations has been done. That volume varies from a profile to another as follow: (P1) from10.1 to 16.3 km^3, (P2) from 0.7 to 8.7 km^3, (P3) from 1.2 to 18 km^3. Based on the present investigation, it is recommended to proceed by: (1) flying the area with a tied grid (aeromagnetic flying space line and nominal clearance respectively less than 300 m and 150 m); (2) designing a drilling grid of 150 m x 150 m and use 3D modeling in order to evaluate the iron formations resources at the stage of measured or proven reserves. In this case, the drilling origin has to be fixed close to the top of each identified iron formations anomaly and the drilling dip has to be determined from the 3D cross section of each anomaly.

Acknowledgements

References

Bessoles, B. and R. Trompette, 1980. Géologie de l'Afrique. La chaîne panafricaine: "zone mobile" d'Afrique Centrale (partie sud) et "zone mobile" soudanaise. *Mémoires du Bureau de Recherches Géologiques et Minières (BRGM)*, **92**, 396 p.

Bhattacharyya, B.K. 1978.Computer modeling in gravity and magnetic interpretation. *Geophysics*, **43**, 5, 912–929.

Boukeke, D.B. 1994. Structures crustales d'Afrique centrale déduite des anomalies gravimétriques et magnétiques: le domaine précambrien de la République Centrafricaine et du Sud-Cameroun, Thèse de Doctorat, université de Paris Sud, 264 p.

Cahen, L., N.J. Sneling, J. Delhal and J.R. Vail, 1984.The geochronology and evolution of Africa. *Clarendon Press*, Oxford, 512 p.

Champetier de Ribes, G. 1956. Note explicative sur la feuille Yaoundé-Est de la carte géologique de reconnaissance. *Bul. Dir. Mines & Géol. du Cameroun*, 29 p.

Cooper, G.R.J. 1997. Forward modeling of magnetic data. *Computer & Geosciences*, **23**(10), 1125–1129.

Eno-Belinga, S.M. 1984. Géologie du Cameroun. *Université de Yaoundé (Cameroun),* 307 p.

Gazel, J. and C. Guiraudie, 1965. Notice explicative sur la région Abong-Mbang Ouest de la carte géologique de reconnaissance. *Bul. Dir. Mines & Géol. du Cameroun*, **5**, 29 p.

Gerard, A. and N. Debeglia, 1975. Automatic three-dimensional modeling for the interpretation of gravity or magnetic anomalies. *Geophysics*, **40** (6), 1014–1034.

Gerard, A. and P. Griveau, 1972. Quantitative interpretation of gravity or magnetic fields from transformed maps of the fields' first vertical derivative. *Geophysical Prospecting*, **20** (2), 459–481.

Grant, F.S. and G.F. West, 1965. Interpretation theory in applied geophysics. Mc Graw-Hill, Book Co., Inc., New York, 584 p.

Gunn, P.J. and M.C. Dentith, 1997. Magnetic responses associated with mineral deposits. *Journal of Australian Geology & Geophysics,* **17**(2), 145–158.

Kaftan, I., S. Mujgan and S. Coskun, 2005. Application of the finite element method to gravity data case study: Western Turkey. *Journal of Geodynamics*, **39**, 431–443.

Kerr, T.L., A.P. O'Sullivan, D.C. Podmore, R. Turner and P. Waters, 1994. Geophysics and iron ore exploration: examples from the Jimblebar and Shay Gap-Yarrie regions, Western Australia. *Australian Society of Exploration Geophysicist, Special Publication*, **7**, 355–368.

Mallick, K. and K.K. Sharma, 1999. A finite element method for computation of the regional gravity anomaly. *Geophysics*, **64**, 461–469.

Mallick, K. and K.K. Sharma, 1997. Computation of regional gravity anomaly- A novel approach. *Proc. Indian Acad. Sci. (Earth planet Sci.),* **106**, 55–59.

Mvondo, H., S. Owona, J. M. Ondoa and J. Essono, 2007. Tectonic evolution of the Yaoundé segment of the Neoproterozoic Central African Orogenic Belt in southern Cameroon. *Can. J. Earth Sci.,* **44**, 433–444.

Ndougsa-Mbarga, T., M. Bikoro-Bi-Alou, C.T. Tabod and K. Kant-Sharma, 2013. Filtering of gravity and magnetic anomalies using the finite element approach (fea). *Journal of Indian Geophysical Union,* **17**(2) in press.

Nédélec, A., J. Macaudière, J.P. Nzenti and P. Barbey, 1986. Evolution métamorphique et structurale des schistes de Mbalmayo (Cameroun) Implications pour la structure de la zone mobile panafricaine d'Afrique centrale, au contact du craton du Congo. Comptes Rendus de l'Académie des Sciences, **303**, 75–80.

Nguimbous-Kouoh, J.J., T. Ndougsa-Mbarga, P. Njandjock-Nouck, A. Eyike, J. O. Campos-Enriquez and E. Manguelle-Dicoum, 2010. The structure of the Goulfey-Tourba sedimentary basin (Chad-Cameroon): a gravity study. *Geofísica Internacional*, **49** (4), 181–193.

Njandjock, P., E. Manguelle-Dicoum, T. Ndougsa-Mbarga and C. T. Tabod, 2006. Spectral analysis and gravity modelling in the Yagoua, Cameroon, sedimentary basin. *Geofísica Internacional*, **45**(2), 209–215.

Nnange, J.M., V. Ngako, J.D. Fairhead and C.J. Ebinger, 2000. Depths to density discontinuities beneath the Adamawa Plateau region, Central Africa, from spectral analysis of new and existing gravity data. *Journal of African Earth Sciences*, **30**(4), 887–901.

Nzenti, J.P., P. Barbey, J. Macaudiere and D. Soba, 1988. Origin and Evolution of the Precambrian high grade Yaoundé gneiss (Cameroon). *Precambrian Res.,* **38**, 91–109.

Olinga, J.B., J.E. Mpesse, D. Minyem, V. Ngako, T. Ndougsa-Mbarga and G.E. Ekodeck, 2010. The Awaé-Ayos strike-slip shear zones (southern Cameroon): Geometry, kinematics and significance in the late Pan-African tectonics. *N. Jb. Geol. Paläont. Abh.* **257**(1), 1–11.

Pal, P.C., K.K. Khurana and P. Unnikrishnan, 1978/79. Two examples of spectral approach to source depth estimation in gravity and magnetic. *Pageoph*, **117**, 772–783.

Parasnis, D.S., 1997. Principles of Applied Geophysics. 5th edition Chapman and Hall, London, England, 400 p.

Paterson, Grant and Watson Ltd., 1976. Interpretation of an aeromagnetic survey over part of the United Republic of Cameroon. ACDI Toronto, 190 p., 39 fig., 2 tables.

Penaye, J., S.F. Toteu, W.R. Van Schmus and J.P. Nzenti, 1993. U-Pb and Sm-Nd preliminary geochronologic data on the Yaoundé Series, Cameroun: re-interpretation of the granulitic rocks as the suture of collision in the Central African Belt. *C.R. Acad. Sci.,* Paris, **317**(2), 789–794.

Shang, C.K., M. Satir, W. Siebel, E.N. Nsifa, H. Taubald, J.P. Liégeois, F.M. Tchoua, 2004. TTG magmatism in the Congo Craton: a view from major and trace element geochemistry, Rb–Sr and Sm–Nd systematics: case of the Sangmelima region, Ntem complex, southern Cameroon. *Journal of African Earth Sciences*, **40**, 61–79.

Spector, A. and F.S. Grant, 1970. Statistical models for interpreting aeromagnetic data. *Geophysics*, **35**(2), 293–302.

SRK Consulting (UK) Limited, 2011. Report on mineral resource estimate for the Nkout iron ore project, community of Djoum, Cameroon. Unpublished report, 128 p.

Suh, C., A. Cabral, E. Ndime, 2009. Geology and ore fabrics of the Nkout high-grade haematite deposit, southern Cameroon. *Society for geology applied to mineral deposits. Smart Science for Exploration and Mining" P. J. Williams et al. (editors)*, 558–563.

Tadjou, J.M., R. Nouayou, J. Kamguia, H.L. Kande and E. Manguelle-Dicoum, 2009. Gravity analysis of the boundary between the Congo craton and the Pan-African belt of Cameroon. *Austrian Journal of Earth Sciences*, **102**, 71–79.

Talwani, M. and J. R. Heirzler, 1964. Computation of magnetic anomalies caused by two-dimensional bodies with application to the Mineral Industry shape. *Computers in the Mineral Industry, School of Eath Sciences, Standford University (Public),* 464–480.

Tchameni, R., K. Mezger, N.E. Nsifa and A. Pouclet, 2001. Crustal origin of Early Proterozoic syenites in the Congo Craton (Ntem complex), South Cameroon. *Lithos*, **57**, 23–42.

Toteu, S.F., J. Penaye and Y.D. Poudjom, 2004. Geodynamic evolution of the Pan-African belt in Central Africa with special reference to Cameroon. *Can. J. Earth Sci.,* **41**, 73–85.